Short-wave and long-wave surface radiation budgets in GCMs: a review based on the IPCC-AR4/ CMIP3 models

Short-wave and long-wave surface radiation budgets in GCMs: a review based on the IPCC-AR4/CMIP3 models

Martin Wild

TELLUS

Short-wave and long-wave surface radiation budgets in GCMs: a review based on the IPCC-AR4/CMIP3 models

By M A R T I N   W I L D *,   *Institute for Atmospheric and Climate Science, ETH Zurich, Universitätsstr. 16, CH-8092 Zurich, Switzerland*

ABSTRACT

Here I review the developments in the representation of radiation budgets in global climate models (GCMs) from a surface perspective, considering early models up to the latest model generation used in the IPCC fourth assessment report (AR4). As in previous model generations, considerable differences in the simulated global mean radiation budgets are also present in the IPCC-AR4 models, particularly in the atmosphere and at the surface. I use a comprehensive set of surface observations to constrain these uncertainties, and focus on the downward short- and long-wave radiation, which can directly be validated against the surface observations. The majority of the IPCC-AR4 models still shows a tendency to overestimate the short-wave and underestimate the long-wave downward radiation at the surface, each by 6 W m^{-2} on average, a long standing problem in many GCMs. A subset of models, however, is now capable of simulating at least one of the short- or long-wave downward components adequately. Model biases in all- and clear-sky fluxes are often similar, suggesting that deficiencies in clear-sky radiative transfer calculations are major contributors to the excessive surface insolation in many of the models. No indication is found that the simulated excessive surface insolation is due to missing cloud absorption.

1. Introduction

The most powerful tools available to quantify and predict the consequences of human interference with climate are three-dimensional general circulation models (GCMs). Anthropogenic climate change is, from a physical point of view, first of all a perturbation of the Earth radiation balance through human emission of greenhouse gases and aerosol. If these perturbations ought to be realistically simulated, it is an essential pre-requisite that the components of the Earth radiation balance are adequately reproduced in these models.

Validation studies have traditionally been focusing on the GCMs' radiation balance at the top of atmosphere (TOA), where satellite observations can be used as constraints. Much less emphasis has been placed on the radiation balance at the surface, where no similar observational constraints have been available for comparison.

The aim of the present paper is, therefore, to review and document the developments in radiation budget modelling in GCMs from a surface perspective over the last few decades, up to the latest generation of GCMs used in the 4th assessment report of the Intergovernmental Panel on Climate Change (IPCC-AR4, IPCC, 2007). The focus is on the radiative fluxes in both the short-wave (also known as solar, 0.2–4 μm) and long-wave (also known as thermal or terrestrial, 4–100 μm) part of the electromagnetic spectrum.

2. Representation of surface radiation balance in GCMs: a historic perspective

A first attempt to compare the surface radiation balance in different GCMs has been made by Gutowski et al. (1991), who found substantial discrepancies among the surface energy balance components in three GCMs representative of the late 1980s. Randall et al. (1992) noted in a sensitivity experiment with an imposed global increase in sea surface temperature of 4 K significant differences in the simulated surface energy balance changes in 19 GCMs.

First attempts to evaluate components of the surface radiation balance against direct surface observations on a worldwide basis were made by Garratt (1994) for the downward short-wave and Wild et al. (1995) for the downward short-wave, long-wave and net radiation. It was shown in these studies, that the evaluated GCMs had a strong tendency to overestimate the downward solar radiation compared to worldwide distributed surface observations (22 sites in Garratt, 1994, 760 sites in Wild et al., 1995). Excessive surface insolation in several GCMs was also reported in studies using satellite-derived estimates of surface irradiance as reference (Li et al., 1997), as well as in various more recent studies focusing on individual GCMs or regional climate models (e.g. Morcrette, 2002a; Bodas-Salenco et al., 2008; Marcovic et al., 2008).

Wild et al. (1995), based on a stand alone validation of a GCM radiation code, showed that the excessive insolation is also present under cloud free conditions, pointing to an underestimation of absorption of solar radiation in the cloud free atmosphere. An excessive surface insolation under cloud-free conditions was also found in other radiation codes (e.g. Kato et al., 1997; Kinne et al., 1998; Wild and Liepert, 1998; Wild, 2000; Morcrette, 2002a; Wild et al., 2006). Wild et al. (1995, 1998a) suggested that the excessive insolation is related to an underestimation of water vapour absorption in the GCM radiation codes, in line with evidence from radiation code intercomparison projects (Fouquart et al., 1991). It was also shown that models with higher water vapour absorption from updated spectroscopic data are in better agreement with the surface observations (Wild et al., 1998a,b, 2006). More recently, Cagnazzo et al. (2007) suggested that ozone absorption can also be underestimated in GCM codes with broad bands in the short-wave, thereby contributing to excessive surface insolation as well. Haltore et al. (2005) showed, that also the diffuse fraction of the clear-sky surface solar flux is overestimated in several radiation codes of different complexity.

Other studies suggested that absorption of solar radiation in clouds may be considerably larger than assumed in the models (Cess et al., 1995; Ramanathan et al., 1995), which would offer another explanation for the excessive surface insolation in the models. This issue has also become known as the 'anomalous absorption phenomenon' and has lead to controversial discussions (e.g. Cess et al., 1995; Ramanathan et al., 1995; Li et al., 1995, 1999; Wild et al., 1998a; Arking, 1999; Wild, 2000; Ackerman et al., 2003).

A part of the excessive surface insolation has also been related to an inadequate representation or an entire lack of aerosol in some of these earlier models (e.g. Cusack et al., 1998; Wild, 1999; Haltore et al., 2005; Wild et al., 2006). It was further shown that the biases were particularly large in areas with high aerosol loadings, such as in regions with strong biomass burning (Wild, 1999). Cusack et al. (1998) showed that the introduction of a simple aerosol climatology can already significantly reduce the biases in surface insolation compared to a simulation with no aerosol effects included.

In an analysis of 20 GCMs, taking part in the second phase of the Atmospheric Model Intercomparsion Project (AMIP II), representative for the state of climate modelling at the end of the 1990s, Wild (2005) pointed out that the GCMs continued to overestimate the insolation at the surface, by 9 W m^{-2} on average, compared with a comprehensive set of worldwide distributed observation sites. The biases of the solar fluxes at the top of atmosphere compared with satellite observations were found to be generally much smaller. This suggests that the excessive surface solar radiation in many of the GCMs was rather related to inaccurate partitioning of solar absorption between atmosphere and surface than to excessive absorption by the planet as a whole. The excessive surface insolation in the GCMs was also shown to have a major detrimental impact on the simulation of the surface climate and, for example, contributed significantly to the problem of excessive summer dryness over continental surfaces (Wild et al., 1996). This has been a well-known and long-standing problem in many GCMs.

The representation of the energy exchange between the surface and atmosphere in the long-wave spectral range in GCMs has first been assessed in Wild et al. (1995). Therein it was shown that GCMs at the time underestimated the downward long-wave radiation at the surface by 10–15 W m^{-2}. Such an underestimate in downward long-wave radiation is comparable in magnitude to the expected change in this quantity in scenarios with doubled carbon dioxide concentration, as pointed out in Wild et al. (1997). An underestimation of downward long-wave radiation was also noted in follow up studies by Garratt and Prata (1996) and Wild et al. (2001), as well as in a number of more recent studies focusing on other individual GCMs or regional climate models up to the present day (e.g. Bodas-Salenco et al., 2008; Marcovic et al., 2008). The underestimation was shown to be mainly due to a lack of thermal emission of the cloud-free atmosphere (Dutton, 1993; Wild et al., 1995, 2001; Chevallier and Morcrette, 2000; Marcovic et al., 2008). Wild et al. (1998a, 2001) further presented evidence that the simulated downward long-wave radiation was particularly underestimated at higher latitudes with cold dry climates, whereas less so or even overestimated under warm moist climates at low latitudes, in line with the findings of Allan (2000). More recent improvements in the parametrization of the water vapour continuum were shown to reduce this bias (Iacono et al., 2000; Wild et al., 2001; Morcrette, 2002b; Wild and Roeckner, 2006). All the above studies were based on individual or a few different models only. No evaluation of the downward long-wave radiation in an extended set of models has been published so far. This will be resumed here, starting from the AMIP II model intercomparison project (models representative of the late 1990s) up to the current generation of models used in IPCC-AR4.

The tendency for excessive downward solar radiation and, at the same time, lack of downward long-wave radiation often found in GCMs have lead over many years to a superficially correct simulation of surface net radiation due to error cancellation, as pointed out in Wild et al. (1995, 1998a). In the following section, I investigate to what extent these tendencies remain in the latest generation of GCMs.

3. Representation of surface radiation balance in the IPCC-AR4/CMIP3 GCMs

For the assessment of the latest generation of GCMs participating in the experiments for IPCC-AR4, radiative fluxes of 14 GCMs were available from the program for climate model diagnosis and intercomparison (PCMDI). This experimental framework is also known as CMIP3 (Coupled Model Intercomparison Project). The 14 models included are from NCAR (model versions ccsm3 and pcm1), GFDL (cm2), GISS (e_r, e_h, aom), CCSR (MIROC3_2 medium and high resolution), MRI (cgcm2), UKMO (hadcm3), MPI (echam5), CNRM (cm3), IAP (fgols1) and INM (cm3). For more information on these models, the reader is referred to the web pages of PCMDI (http://www-pcmdi.llnl.gov/). For the present analysis, surface radiative fluxes from these models were extracted as averages over the last decade of the '20th century all forcings' runs. Even though some of the observations used as reference do also stem from the 1980s, this is not critical, as the decadal variations in the GCM surface fluxes are small, with flux differences less than 1 W m^{-2} between the 1980s and the 1990s.

In addition, for the analysis of the long-wave fluxes, 20 models of the earlier generation of GCMs from the Atmospheric Model Intercomparison Project phase 2 (AMIP II) are included in this study as reference.

The observational data for the assessment of the GCM-radiative fluxes have been retrieved from two databases: the Global Energy Balance Archive (GEBA, Ohmura et al., 1989; Gilgen et al., 1998) and the database of the Baseline Surface Radiation Network (BSRN, Ohmura et al., 1998). GEBA is a database for the worldwide measured energy fluxes at the Earth's surface and currently contains 2000 stations with 250000 monthly mean values of various surface energy balance components. Gilgen et al. (1998) estimated the relative random error (root mean square error / mean) of the incoming short-wave radiation values in the GEBA at 5% for the monthly means and 2% for yearly means. BSRN provides radiation measurements with the highest possible accuracy at high temporal resolution (minute values) at a limited number of sites (35 to date) in various climate zones. The accuracy of downward long-wave radiation measurements according to BSRN standards is set to 3 W m^{-2} (Ohmura et al., 1998).

3.1. Short-wave radiation

All-sky short-wave radiation budgets at the TOA, within the atmosphere and at the surface for 13 of the IPCC-AR4/CMIP3 models are shown in Fig. 1. Not included in this figure is the NCAR PCM1 model, with a surface absorption of 173 W m^{-2}, but where no TOA fluxes were available to calculate atmospheric and TOA budgets. In the upper panel of Fig. 1, the short-wave radiation balance at the TOA of the various models is shown, which corresponds to the total amount of solar energy absorbed within the climate system. This amount varies in a range of 10 W m^{-2} between the models, with the median model value close to the satellite estimate from the Earth Radiation Budget Experiment (ERBE) of 240 W m^{-2}. The good agreement between simulated and observed value is not surprising, since models are typically tuned in their cloud schemes to match the satellite observed values on a global mean basis. More difficult for the models is the partitioning of this total absorbed energy between atmospheric and surface absorption (middle and lower panel of Fig. 1), where no such tuning has been applied. Accordingly, the model ranges of atmospheric and surface absorption (15 and 23 Wm^{-2}, respectively) are substantially larger, despite their smaller absolute values. In relative terms, atmospheric and surface model ranges cover 20% and 14% of their absolute values, respectively, whereas the model range of TOA values covers only 4% of their absolute values. Thus, also the IPCC-AR4/CMIP3 models, as their preceding model generations (*cf.* Section 2), show still a considerable spread in their surface and atmospheric radiation budgets.

Observation-based estimates on global mean atmospheric and surface absorption also show large discrepancies and are not necessarily close to the median or mean model values. As an example, estimates of atmospheric and surface short-wave absorption derived in Wild et al. (1998a) are added for comparison in Fig. 1. These estimates indicate a higher atmospheric and lower surface absorption than found in most models.

To get further insight into these discrepancies, we can compare the surface fluxes calculated in the models with the observations stored in GEBA. For a direct comparison with the available measurements, I use the downward component of the short-wave flux at the surface, rather than the absorbed shown in Fig. 1, since the downward flux can directly be compared to measurements. For the comparison, I use the 760 worldwide distributed stations shown in Fig. 2. The station distribution is the same as in Wild (2005) to allow for a direct comparison of the results obtained here with the IPCC-AR4 models with the results in Wild (2005) with the former generation AMIP II models. The model data were interpolated to the measurement sites using the four surrounding gridpoints, weighted by their inverse spherical distance. It can be argued that a comparison of GCM results with point observations may not be representative due to the subgrid variability. However, it is not the aim of this work to concentrate on specific locations but on the general trend at
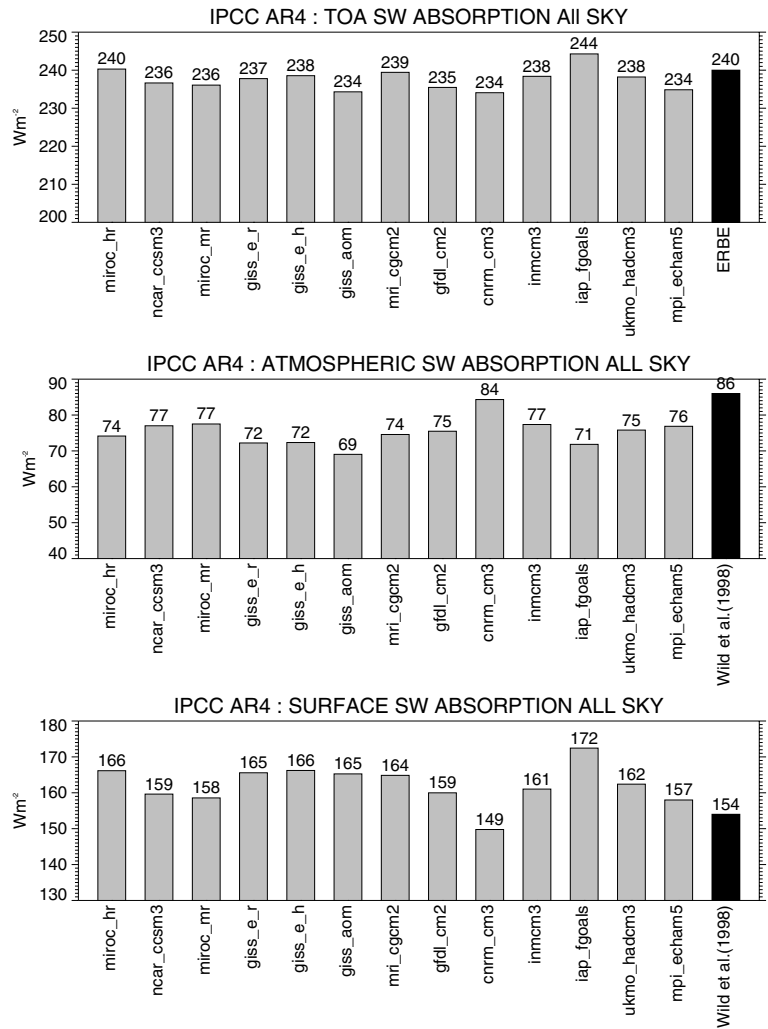
IPCC AR4 : TOA SW ABSORPTION All SKY

IPCC AR4 : ATMOSPHERIC SW ABSORPTION ALL SKY

IPCC AR4 : SURFACE SW ABSORPTION ALL SKY

Fig. 1. Global mean surface, atmosphere and top-of atmosphere short-wave radiation budgets in the various IPCC-AR4/CMIP3 GCMs. Observational references from the Earth Radiation Budget Experiment (ERBE, Barkstroem et al., 1990) and from Wild et al. (1998a).
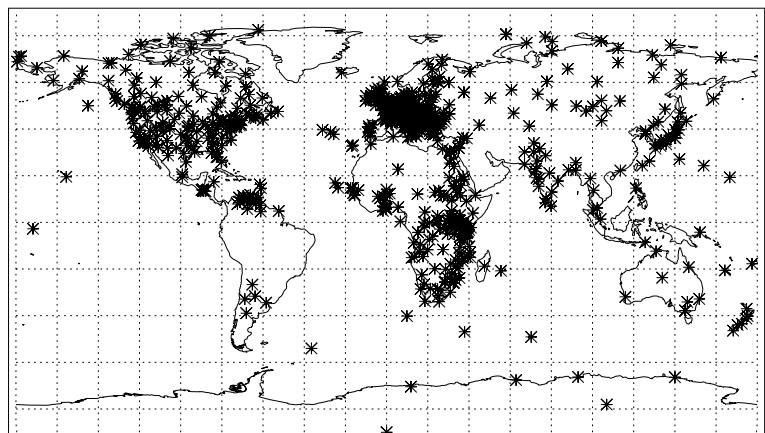

Fig. 2. Geographical distribution of 760 observation sites with extended records of downward short-wave radiation as available from GEBA.

a large number of sites, which should not be systematically affected by local deviations. Long-term annual mean short-wave downward radiation observed at the 760 sites are compared with the corresponding fluxes calculated by the various IPCC-AR4 GCMs in Fig. 3. Overall the calculated downward surface fluxes correlate well with their observed counterparts, with correlation coefficients ranging from 0.89 to 0.94. However, the high correlation is favoured by the common dependence of both observed
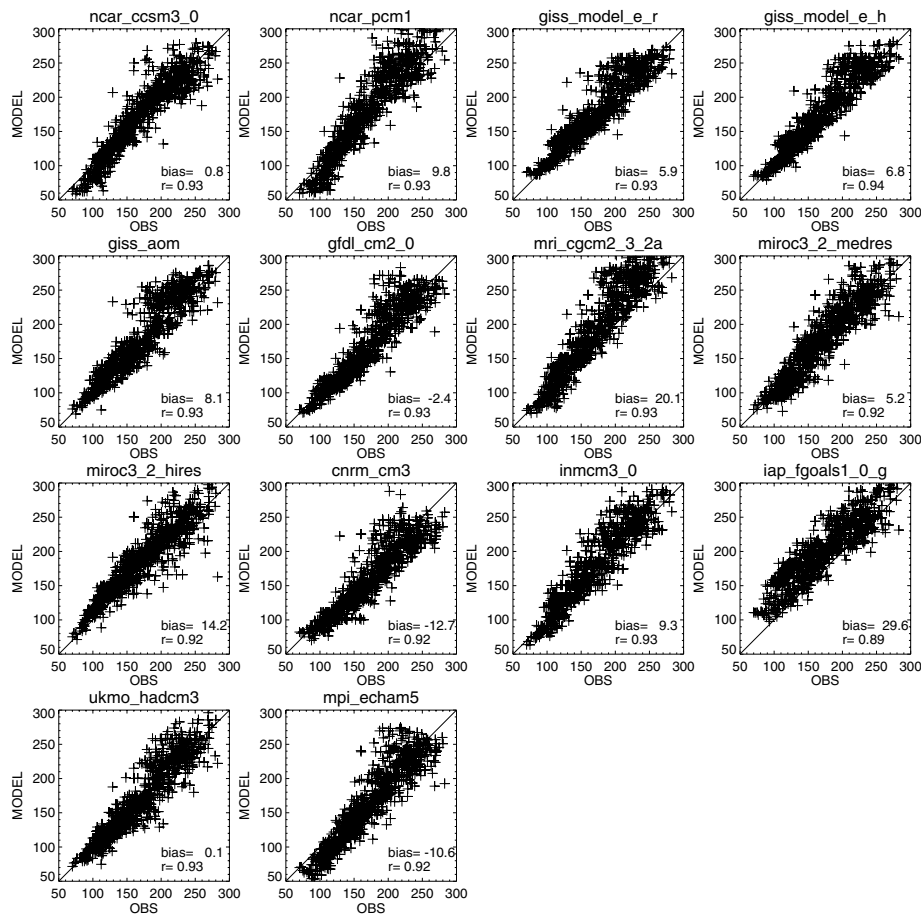
Fig. 3. Long-term mean downward short-wave radiation calculated by the various IPCC-AR4/CMIP3 GCMs and observed at 760 sites from GEBA (Units $W\,m^{-2}$).

and calculated fluxes on the incoming solar radiation at the TOA with large latitudinal variation.

Mean model biases averaged over all 760 stations range between $+29.6$ and -12.7 $W\,m^{-2}$ (Table 1, first column, and Fig. 3), with a model mean bias of $+6$ $W\,m^{-2}$. Out of the 14 models, 11 tend to overestimate the surface insolation, whereas 3 tend to underestimate this quantity. The excessive surface insolation, this long standing problem in GCMs (see Section 2), is therefore still present in a majority of the models participating in IPCC-AR4. The overall average bias has been somewhat reduced from $+8.6$ $W\,m^{-2}$ in the former generation model intercomparison AMIP II (Wild, 2005) to $+6.0$ $W\,m^{-2}$ in the present intercomparison for IPCC-AR4 (see Table 2). Note that IPCC-AR4 also includes some newcomer models not participating in prior model intercomparison projects, which may not represent state of the art modelling. Comparing just the models series from those modelling centres where I had data from both AMIP II and IPCC-AR4 intercomparisons (ncar, giss, cnrm, ccsr, ukmo and mpi), the model bias is reduced from $+4.5$ to $+2.7$ $W\,m^{-2}$. Also, there are now a number of models that show an excellent overall agreement with the GEBA observations (Table 1, Fig. 3), such as

ncar_ccsm3 (mean bias $+0.8$ $W\,m^{-2}$), gfdl_cm2_0 (mean bias -2.4 $W\,m^{-2}$) or ukmo_hadcm3 (mean bias 0.1 $W\,m^{-2}$). Thus, progress in modelling of solar radiation under all-sky conditions can be noted particularly in some of the leading modelling centres. In an earlier study (Wild et al., 2006), we specifically looked at clear-sky solar fluxes in the IPCC-AR4 models. Their overall biases compared to surface solar clear-sky climatologies, derived from a selection of BSRN sites, are reproduced in Table 1 for reference. An inspection of the clear- and all-sky biases in Table 1 suggests that models with high all-sky biases also tend to have high clear-sky biases, whereas those models with excellent agreement under all-sky conditions also show very small biases in their clear-sky fluxes. This suggests that all sky biases are, to a large extent, caused by problems in the simulated clear-sky fluxes and not only due to problems in the simulation of cloud radiative effects. This confirms earlier findings pointing to the importance of adequate clear-sky computations for a realistic simulation of the amount of solar radiation at the surface, as outlined in Section 2.

Figure 4 illustrates the global mean short-wave cloud radiative forcing calculated by the IPCC-AR4/CMIP3 models at the TOA,

Table 1. Mean bias in surface downward short-wave radiation of the IPCC-AR4/CMIP3 models determined at 760 worldwide distributed observation sites from GEBA (long-term mean all-sky conditions; Column 1)

Model	All-sky bias	Clear-sky bias (Wild et al., 2006)
ncar-ccsm3	+0.8	+0.7
ncar-pcm1	+9.8	n.a.
giss-er	+5.9	+9.0
giss-eh	+6.8	+5.6
giss-aom	+8.1	n.a.
gfdl-cm2.0	−2.4	−3.9
mri-cgcm2	+20.1	n.a.
miroc-mr	+5.2	+8.1
miroc-hr	+14.2	+8.2
cnrm-cm3	−12.7	−4.7
inmcm3	+9.3	−3.3
iap-fgols1	+29.6	+8.5
ukmo-hadcm3	+0.1	−0.8
mpi-echam5	−10.6	−7.3
multimodel mean bias	+6.0	

Note: For reference, mean model biases for the same quantity but under cloud-free conditions averaged over worldwide distributed BSRN stations are reproduced from Wild et al. (2006) (Column 2; Units W m^{-2}).

Table 2. Mean bias in downward short-wave and long-wave radiation, as well as total (sum of short- and long-wave) downward radiation at the surface, in the AMIP II and the IPCC-AR4/CMIP3

Model	SW down bias	LW down bias	Total down bias
AMIP II			
ccma	1.1	−17.9	−16.8
ccsr	20.4	−10.8	9.6
cnrm	−3.4	−6.1	−9.5
cola	31.0	−2.4	28.6
dnm	7.1	−10.4	−3.3
ecmwf	−5.8	−10.3	−16.1
giss	3.3	−14.2	−10.9
gla	15.6	−15.3	0.3
jma	20.8	−11.0	9.8
mgo	9.5	1.0	10.5
mri	8.4	0.9	9.3
ncar	8.8	−9.1	−0.3
ncep	15.4	−9.2	6.2
pnnl	16.7	−7.6	9.1
sunya	8.9	−7.8	1.1
ugamp	2.4	−11.0	−8.6
uiuc	7.2	−23.2	−16.1
ukmo	3.0	−11.6	−8.6
yonu	10.1	13.1	23.2
mpi	−9.2	2.1	−7.1
Multimodel mean AMIP II	8.6	−8.0	0.5
IPCC-AR4			
ncar-ccsm3	0.8	−6.9	−6.1
ncar-pcm1	9.8	−7.9	1.9
giss-er	5.9	n.a.	n.a.
giss-eh	6.8	n.a.	n.a.
giss-aom	8.1	6.0	14.1
gfdl-cm2.0	−2.4	−10.4	−12.8
mri-cgcm2	20.1	−10.8	9.3
miroc-mr	5.2	−6.0	−0.8
miroc-hr	14.2	−9.0	5.2
cnrm-cm3	−12.7	−1.9	−14.6
inmcm3	9.3	−0.4	8.9
iap-fgols1	29.6	−9.0	20.6
ukmo-hadcm3	0.1	−10.2	−10.1
mpi-echam5	−10.6	−0.4	−11.0
Multimodel mean IPCC-AR4 (withouth giss-er/rh)	6.0	−5.6	0.4

Note: Biases are determined as averages over 760 sites from GEBA and 44 sites from GEBA/BSRN for the short- and long-wave components, respectively. AMIP II short-wave biases are taken from Wild (2005) (Units W m^{-2}).

in the atmosphere and at the surface, defined as the difference between the corresponding all- and clear-sky fluxes. This figure suggests that cloud radiative forcing at the TOA, compared with ERBE, is generally well simulated in the models. Again, this is partly a consequence of the tuning of the simulated (all-sky) global mean fluxes against the satellite-observed global mean.

When the clear-sky fluxes are well simulated (in those models with comparatively high atmospheric clear-sky absorption, see Wild et al., 2006), I see no necessity for an enhanced or anomalous cloud absorption, as claimed in some studies (see Section 2), to bring the models in agreement with surface observations. This can be inferred from the three models mentioned above, with very small overall biases in both clear- and all-sky surface fluxes. A measure for the overall effect of clouds on the short-wave atmospheric column absorption is the ratio R of short-wave cloud radiative forcing at the surface to that at the TOA (Cess et al., 1995; for limitations of this concept see Li et al., 1995). $R = 1$ states that the presence of clouds does not alter the overall absorption in the atmospheric column. In the controversial discussion of anomalous cloud absorption (see Section 2), published estimates for R vary in a wide range from close to 1.0 (e.g. Li et al., 1995; Wild, 2000) up to 1.5 (e.g. Cess et al., 1995), the latter suggesting a much higher absorption of solar radiation in the cloudy than in the cloud-free atmospheric column. Values of R calculated by the IPCC-AR4 GCMs are given in Fig. 5, determined as ratio of the surface and TOA cloud radiative

forcings given in Fig. 4. All models show R values fairly close to 1, substantially lower than the 1.5 advocated by the studies claiming an anomalous cloud absorption. The three cited models above, with marginal biases in both all- and clear-sky fluxes and
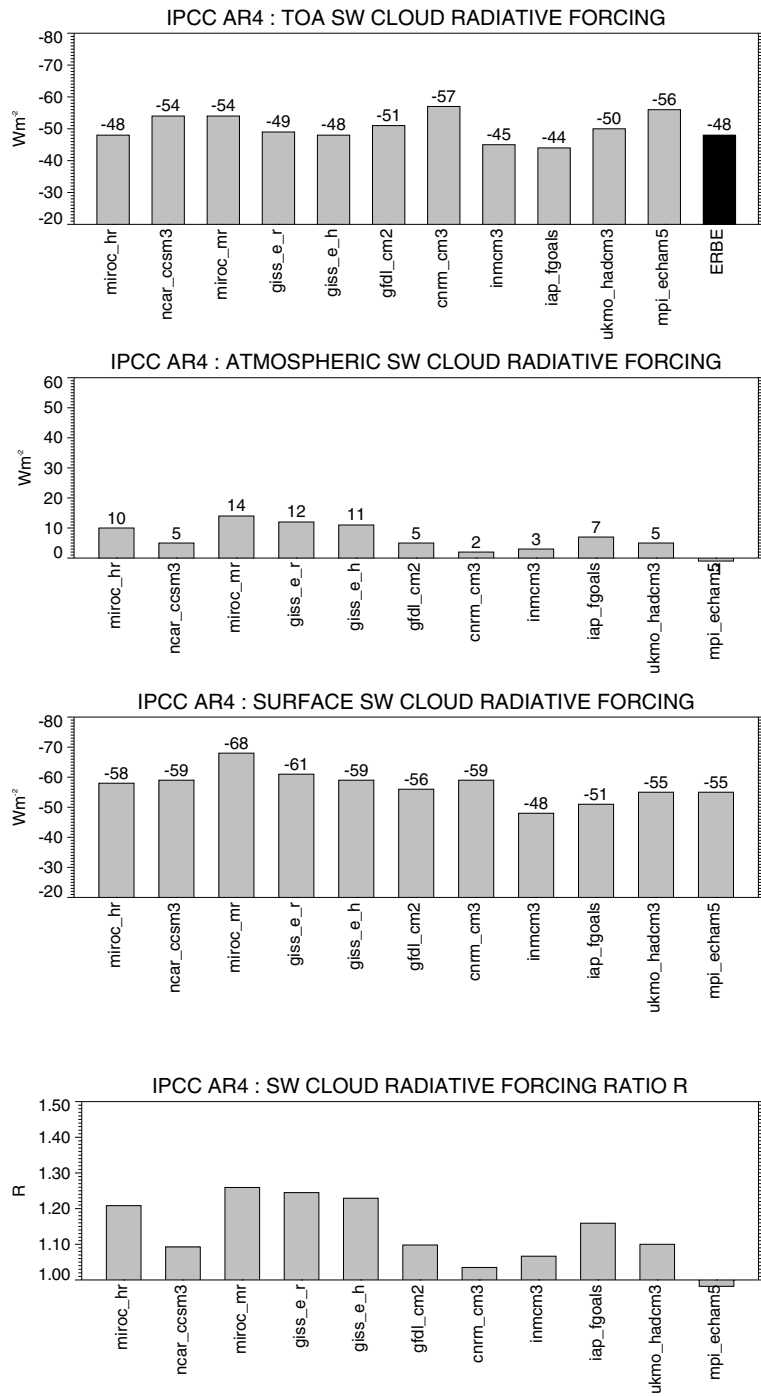
IPCC AR4 : TOA SW CLOUD RADIATIVE FORCING

IPCC AR4 : ATMOSPHERIC SW CLOUD RADIATIVE FORCING

IPCC AR4 : SURFACE SW CLOUD RADIATIVE FORCING

Fig. 4. Global mean surface, atmosphere and top-of atmosphere short-wave cloud radiative forcings (defined as difference between all- and clear-sky fluxes) in the various IPCC-AR4/CMIP3 GCMs. Observational references from the Earth Radiation Budget Experiment (ERBE, Barkstroem et al., 1990).

IPCC AR4 : SW CLOUD RADIATIVE FORCING RATIO R

Fig. 5. Ratio *R* of short-wave cloud radiative forcing at the surface to that at the TOA (long-term global mean) in the IPCC-AR4/CMIP3 GCMs.

thus, by definition, also in the surface and TOA cloud radiative forcing, have *R* values of 1.09 (ncar_ccsm3), 1.10 (gfdl_cm2_0) and 1.10 (ukmo_hadcm3). This implies that the presence of clouds in the state of the art IPCC-AR4 GCMs does not substantially increase the overall absorption of solar radiation in the atmospheric column compared with the cloud-free column. This result gives, therefore, no support for an anomalous or

missing cloud absorption and suggests that no major change in cloud absorption has to be introduced in the models to explain discrepancies between models and surface observations, in line with the findings in Li et al. (1999), Wild (2000) and Ackerman et al. (2003).

In many models, the biases in surface solar radiation show also a characteristic latitudinal structure. This is shown in
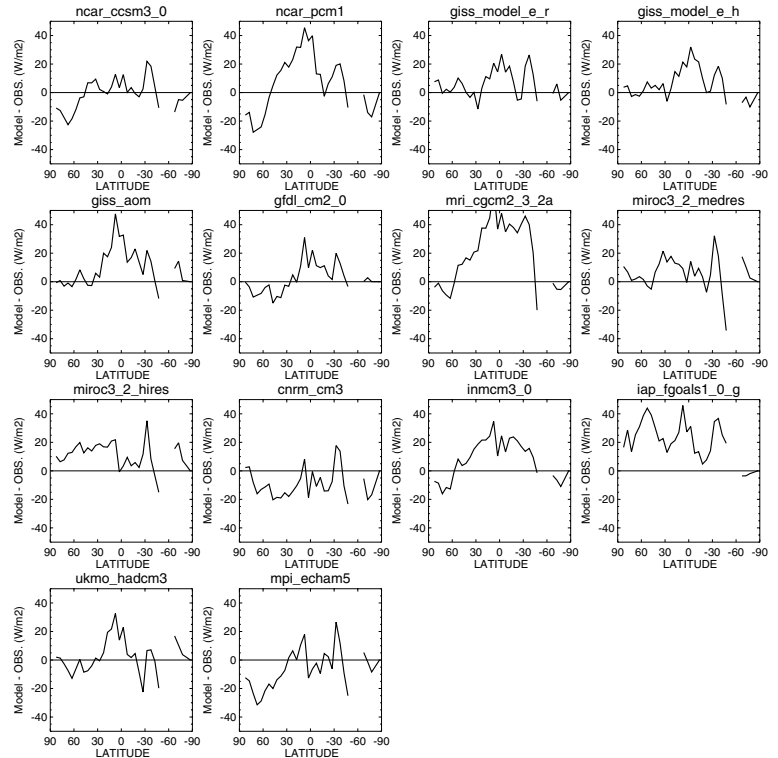
Fig. 6. Model bias of all-sky short-wave downward fluxes at the surface, at 760 observational sites as function of latitude, for various IPCC-AR4 /CMIP3 GCMs. Biases averaged over sites within 5° latitudinal bands. Surface observations from GEBA (Units $W\,m^{-2}$).

Fig. 6, where the model biases have been averaged over the sites located within latitudinal belts of 5°. This figure suggests that overestimates in downward short-wave radiation are particularly pronounced in lower latitudes in a majority of the models. This is in line with evidence from earlier models that a lack of adequate representation of absorbing aerosol, particularly from biomass burning and desert dust prevailing in lower latitudes, can cause significant overestimation in surface insolation (Wild, 1999). Obviously such biases are still present in several of the IPCC-AR4 GCMs.

3.2. Long-wave radiation

The long-wave radiation is of key importance in the context of climate change as it shows an immediate response to changes in atmospheric greenhouse gas concentration. Similarly to the short-wave fluxes, on a global average basis, the long-wave fluxes of the GCMs tend to agree better at the TOA, where they are again tuned to match satellite values, than at the surface, where observational constraints are much weaker. This is evident from Fig. 7, which shows the net surface, atmospheric and TOA long-wave all-sky balances of the IPCC-AR4 models. The outgoing long-wave radiation at the TOA (top panel of Fig. 7) is very similar in the models and varies in a range of $9\,W\,m^{-2}$, or less than 4% of its absolute value, and the mean value of the models ($234\,W\,m^{-2}$) match the ERBE satellite constraint perfectly. The atmospheric and surface balances (middle

and lower panel of Fig. 7), on the other hand, cover both a range of $24\,W\,m^{-2}$, corresponding to 13% and 40% of their absolute values, respectively (Fig. 7). The net long-wave surface balances in the models are also mostly more negative than the estimate given in Wild et al. (1998a). Within the long-wave surface balance, the upward flux can be modelled straightforward, using the model surface temperature and the Stefan Boltzman law, and is therefore affected with less uncertainties. More challenging is, therefore, the modelling of the downward long-wave flux at the surface, which has to take into account the complex physical vertical composition of the atmosphere. The focus in the following is therefore on the downward long-wave flux. Global mean values of downward long-wave radiation in the various models are shown in Fig. 8, for the earlier AMIP II models, and in Fig. 9, for the more recent IPCC-AR4 models. The two figures document the significant spread among the models in this flux in both model intercomparisons. The upper panels in Figs. 8 and 9 present the downward long-wave fluxes under all-sky conditions, whereas the lower panels show the same fluxes under clear-sky conditions. For the all-sky fluxes, in addition, a best estimate of $344\,W\,m^{-2}$, as derived in Wild et al. (2001), is shown as reference. This estimate is $7\,W\,m^{-2}$ higher than the median value of downward all-sky long-wave radiation in the IPCC-AR4 models ($337\,W\,m^{-2}$) and $8\,W\,m^{-2}$ higher than the corresponding median of the AMIP II models ($336\,W\,m^{-2}$). It is interesting to note that the global mean clear-sky fluxes show a larger variability among the models than their all-sky
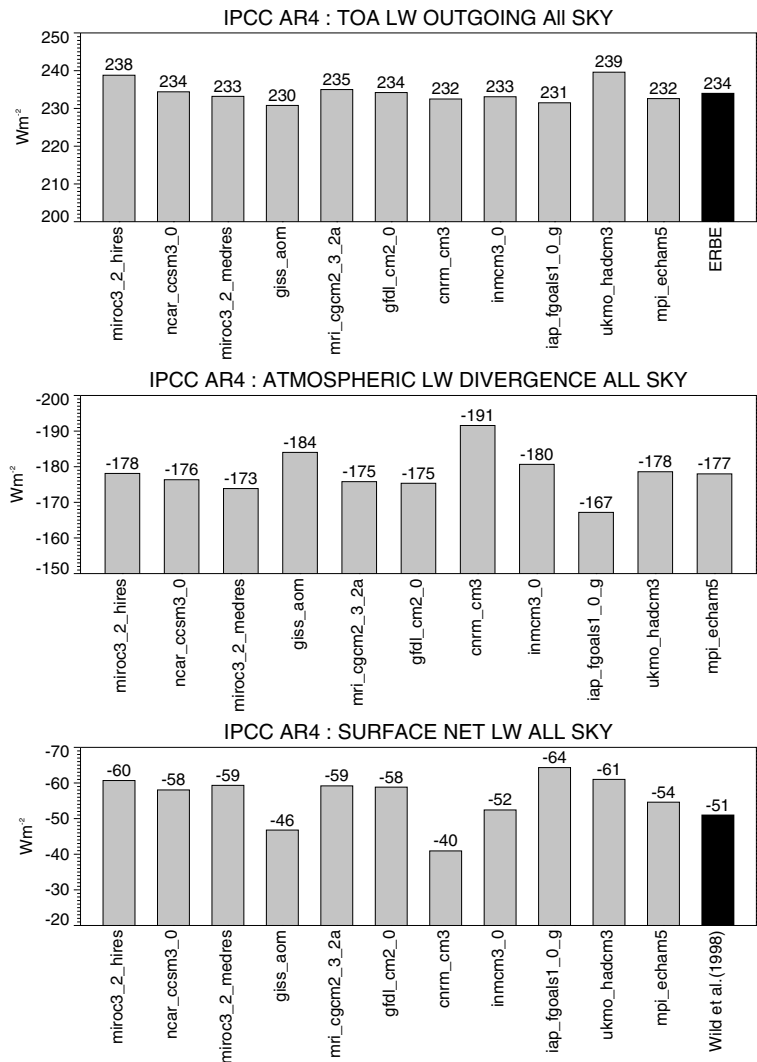
Fig. 7. Global mean surface, atmosphere and top-of atmosphere long-wave balances in the various IPCC-AR4/CMIP3 GCMs. Observational references from the Earth Radiation Budget Experiment (ERBE, Barkstroem et al., 1990) and from Wild et al. (1998a).

counterparts. For example, the standard deviation in the all-sky fluxes of the 20 AMIP II models in Fig. 8 (upper panel) amounts to 7.6 Wm^{-2}, whereas the corresponding *SD* in the clear-sky fluxes (Fig. 8 lower panel) amounts to 9.4 W m^{-2}. A similar effect can be found in the IPCC-AR4 models, with a standard deviation of 5.6 W m^{-2} in the all-sky fluxes and 13.4 W m^{-2} in the clear-sky fluxes (Fig. 9). This indicates that clouds mask, to some extent, the differences in the clear-sky downward long-wave fluxes calculated in the various models and suggests that uncertainties in the long-wave emission of the cloud-free atmosphere is the dominant source of the intermodel differences.

There are less observational constraints for the long-wave fluxes than for their short-wave counterparts since the long-wave radiation is more difficult to measure from the surface than the short-wave radiation and available only at a limited number of sites. The situation has improved to some extent with the establishment of the BSRN, which specifies the downward long-wave radiation as a mandatory measurement in its guidelines. There-

fore, at selected stations in different climate regimes, downward long-wave radiation measurements have become gradually operational since the 1990s. For the present comparison I use, in addition to the downward long-wave radiation measurements contained in GEBA, a selection of records from BSRN. This results in a total of 44 sites available for the comparison, as shown on the map in Fig. 10. A comparison of long-term annual mean downward long-wave radiation as observed and calculated at the 44 sites is shown in Fig. 11 for the AMIP II models and Fig. 12 for the IPCC-AR4 models. Overall, the agreement is fairly well, as reflected in the high correlation coefficients, which are, however, favoured by a strong latitudinal dependence of both modelled and observed fluxes. It is noteworthy that the overall model bias, averaged over the 44 sites, is negative in 16 of the 20 AMIPII models and in 11 of the 12 IPCC-AR4 models included in the analysis (Figs. 11 and 12, Table 2). The underestimation of downward long-wave models is another long standing problem in GCMs, as discussed in Section 2. The multi model
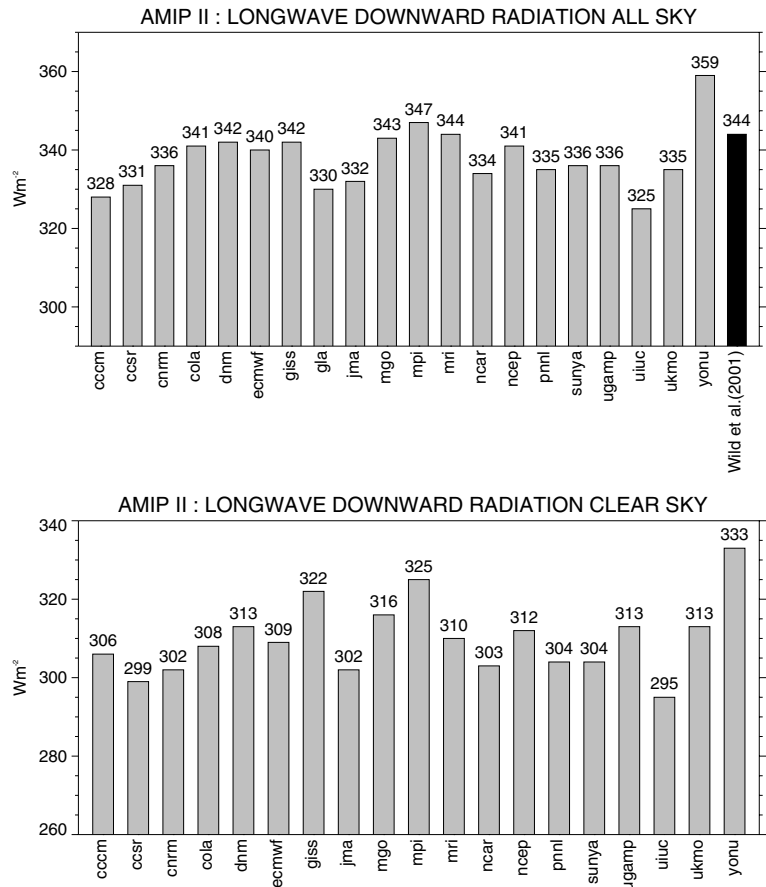
Fig. 8. Global mean downward long-wave radiation at the surface under all-sky (top) and clear-sky (bottom) conditions in the various AMIP II GCMs. Reference value from Wild et al. (2001) (Units W m^{-2}).

mean bias in the IPCC-AR4 models amounts to -5.6 W m^{-2}, which is slightly smaller than in AMIP II (-8 W m^{-2}). Interestingly enough, in both intercomparison projects, the magnitude of this long-wave bias is almost identical, but of opposite sign to the multi mean bias in the short-wave (multimodel mean excess surface solar radiation $+6$ W m^{-2} in the IPCC-AR4 models and $+8.6$ Wm^{-2} in the AMIPII models, see Table 2). This clearly reflects the overall error balance between excessive downward solar and lack of downward thermal radiation, which can be noted in various AMIP II models and still in some of the IPCC-AR4 models, as shown in Table 2. Such error cancellations may lead to a superficially realistic surface radiation balance on a global annual mean basis, but do not apply on regional, seasonal or diurnal scales where the related biases may invoke substantial deficiencies in the simulation of surface climate.

It is noteworthy, however, that as in the short-wave, the bias in downward long-wave radiation has become very small in several of the models. Yet these models (e.g. mpi-echam5), are not identical with the ones that showed negligible biases in the short-wave surface flux. This indicates that most current models still have a problem in the simulation of at least one of the two downward (short- or long-wave) radiative components at the surface.

Improvements in the parametrization of the water vapour continuum can help to remove some of the negative biases in the downward long-wave component (Iacono et al., 2000), as, for example, evidenced for the case of mpi_echam5 in Wild and Roeckner (2006). These improvements appeared to be particularly effective in removing the underestimation in cold dry climates with small absolute flux values (Iacono et al., 2000; Wild and Roeckner, 2006). It is also interesting to note in this respect that in the older AMIP II models, 14 out of 20 models showed in Fig. 11 a linear regression slope less than 1, caused by an underestimation particularly of the fluxes at cold dry sites with small absolute values. These biases are less evident in the more recent IPCC-AR4 models in Fig. 12, pointing to successful updates of the water vapour continuum in some of the models.

4. Summary and conclusions

In this paper I reviewed and documented the developments in short- and long-wave radiation modelling in GCMs over the past decades, up to the latest generation models used in the IPCC 4th assessment report (AR4) and the 3rd phase of the Coupled Model Intercomparison Project (CMIP3). I showed
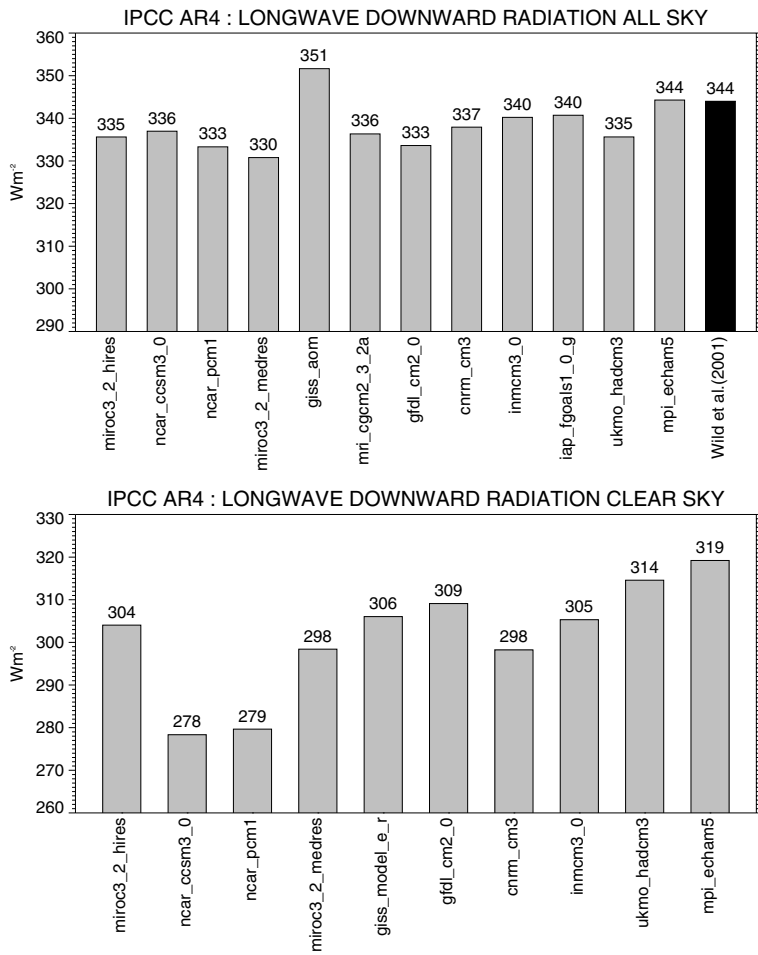
Fig. 9. Global mean downward long-wave radiation at the surface under all-sky (top) and clear-sky (bottom) conditions in the various IPCC-AR4/CMIP3 GCMs. Reference value from Wild et al. (2001) (Units W m^{-2}).
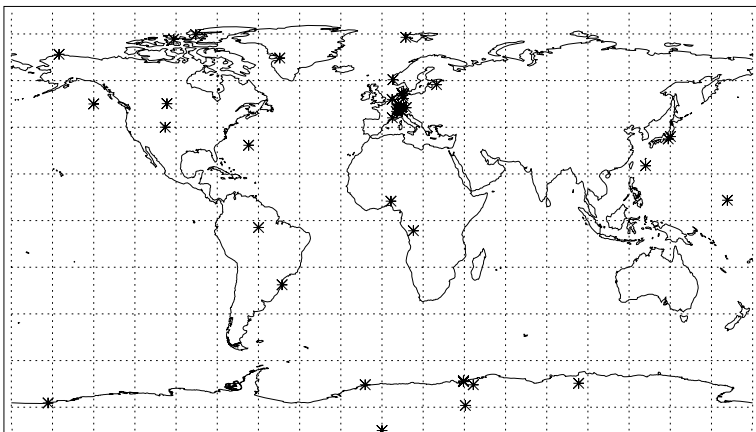

Fig. 10. Geographical distribution of 44 GEBA and BSRN sites with multiannual records of downward long-wave radiation.

that considerable differences still exist, even on a global mean basis, although somewhat reduced compared with earlier model intercomparisons. Compared to a comprehensive set of surface observations, a long standing problem continues to appear in the IPCC-AR4/CMIP3 models: the models still show an overall tendency to overestimate the downward solar radiation and underestimate the downward long-wave radiation at the sur-

face by +6 and −5.6 Wm^{-2}, respectively, on average over all models. The biases are thus qualitatively similar, yet quantitatively smaller compared to earlier model intercomparisons such as AMIP II. In the short-wave, the biases under all-sky conditions are similar to the biases under clear-sky conditions, suggesting that biases are largely influenced by processes in the cloud-free atmosphere. No indication has been found that an
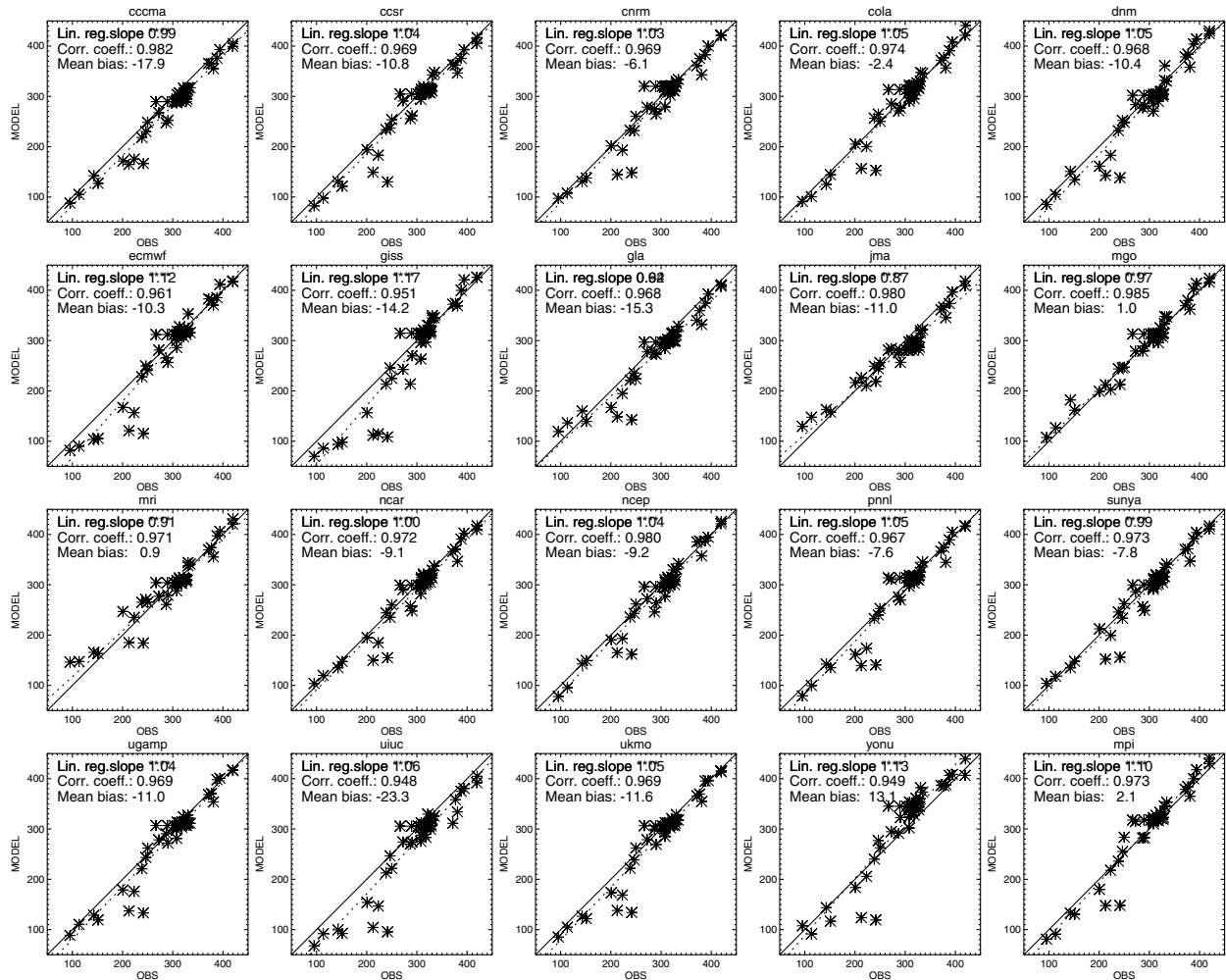
Fig. 11. Long-term mean downward long-wave radiation calculated by the various AMIP II GCMs and observed at 44 sites from BSRN and GEBA (Units W m^{-2}).

enhanced cloud absorption is required in the models to match the observed fluxes. Thus, an 'anomalous' cloud absorption is not supported in this study. There are now a subsection of models that show overall a very small mean bias compared to the surface observations (less than 2 W m^{-2}), at least in one of the two relevant spectral ranges. In the short-wave range, these are the ukmo_hadcm3, gfdl_cm2 and ncar_ccsm3 models, whereas in the long-wave range, for example, the mpi_echam5 model shows a particularly small overall bias. These results provide promising perspectives for the treatment of radiation in GCMs. Still, none of the models is able to simulate both short- and long-wave components adequately. This indicates that there remains room for improvement in most of the current GCMs.

An accurate simulation of the surface radiation budget is an essential pre-requisite for a successful coupling of the atmospheric module to the other components of the climate modelling system, such as the ocean, land surface, biosphere or cryosphere modules. Biases in the GCM radiation budgets may also influence

climate sensitivity, and thereby, potentially distort predictions of future climate states.
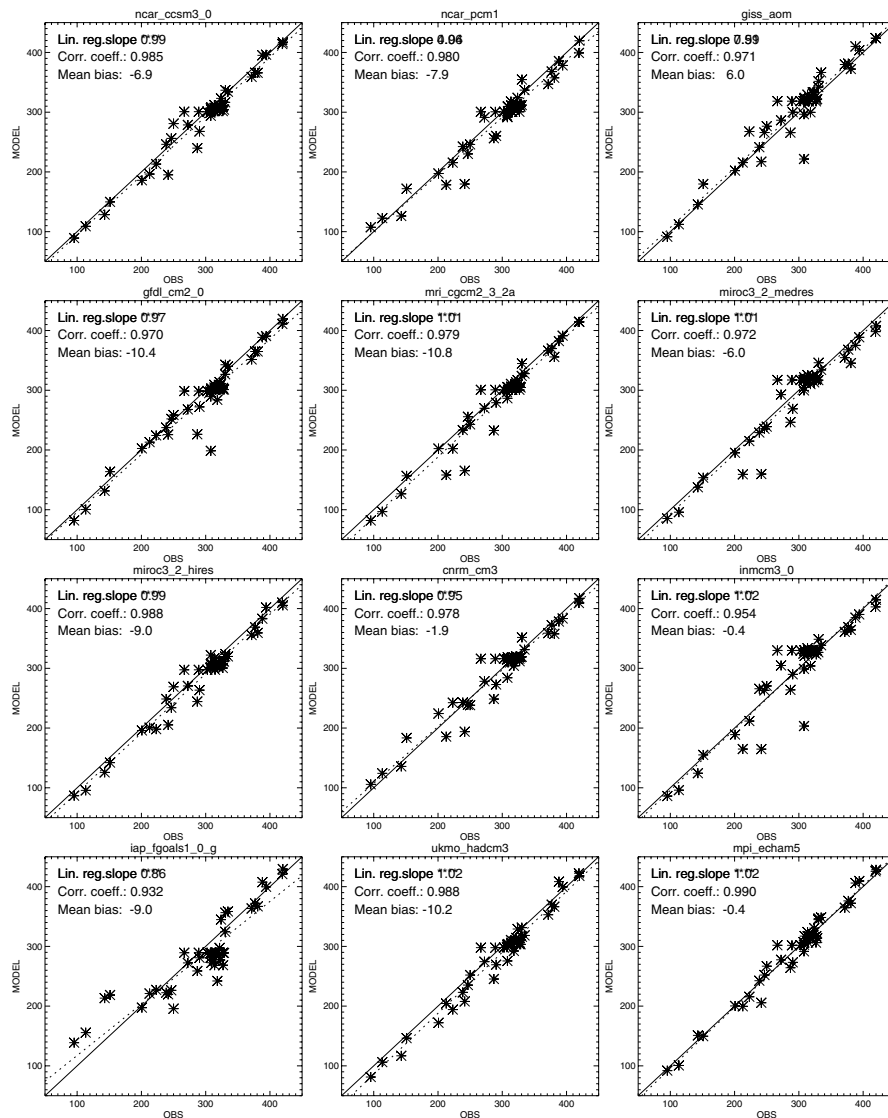
5. Acknowledgments

Fig. 12. Long-term mean downward long-wave radiation calculated by the various IPCC-AR4/CMIP3 GCMs and observed at 44 sites from BSRN and GEBA (Units $W m^{-2}$).

for organizing the model data analysis activity and the IPCC WG1 TSU for technical support. The IPCC Data Archive at Lawrence Livermore National Laboratory is supported by the Office of Science, U.S. Department of Energy. I also would like to take this opportunity to acknowledge many anonymous site scientists in the field, without their dedication this study would not have been possible.

References

Ackerman, T. P., Flynn, D. M. and Marchand, R. T. 2003. Quantifyingh the magnitude of anomalous solar absorption. *J. Geophys. Res.* **108**, 4273, doi:10.1029/2002JD002674.

Allan, R. P. 2000. Evaluation of simulated clear-sky longwave radiation using ground-based observations. *J. Clim.* **13**, 1951–1964.

Arking, A. 1999. The influence of clouds and water vapor on atmospheric absorption. *Geophys. Res. Lett.* **26**, 2729–2732.

Barkstrom, B. R., Harrison, E. F. and Lee, R. B. III 1990. Earth Radiation Budget Experiment. *EOS* **71**, 297–305.

Bodas-Salcedo, A., Ringer, M. A. and Jones, A. 2008. Evaluation of the surface radiation budget in the atmospheric component of the Hadley Centre Global Environmental Model (HadGEM1). *J. Clim.* in press.

Cagnazzo, C., Manzini, E., Giorgetta, M. A., De Forster, P. M. and Morcrette, J. J. 2007. Impact of an improved shortwave radiation scheme in the MAECHAM5 General Circulation Model. *Atmos. Chem. Phys.* **7**, 2503–2515.

Cess, R. D., Zhang, M. H., Minnis, P., Corsetti, X., Dutton, E. G., and co-authors. 1995. Absorption of solar radiation by clouds: observations versus models. *Science* **267**, 496–499.

Chevallier, F. and Morcrette, J. J. 2000. Comparison of model fluxes with surface and top-of-the-atmosphere observations. *Mon. Wea. Rev.* **128**, 3839–3852.

Cusack, S., Slingo, A., Edwards, J. M. and Wild, M. 1998. The radiative impact of a simple aerosol climatology on the Hadley centre atmospheric GCM. *Quart. J. Roy. Met. Soc.* **124**, 2517–2526.

Dutton, E. G. 1993. An extended comparison between LOWTRAN7 computed and observed broadband thermal irradiances: global extreme and intermediate surface conditions. *J. Atmos. Ocean. Technol.* **10**, 326–336.

Fouquart, Y., Bonnel, B. and Ramaswamy, V. 1991. Intercomparing shortwave radiation codes for climate studies. *J. Geophys. Res.* **96**, 8929–8953.

Garratt, J. R. 1994. Incoming shortwave fluxes at the surface – a comparison of GCM results with observations. *J. Clim.* **7**, 72–80.

Garratt, J. R. and Prata, A. 1996. Downwelling longwave fluxes at continental surfaces—a comparison with GCM simulations and implications for the global land-surface radiation budget. *J. Clim.* **11**, 646–655.

Gilgen, H., Wild, M. and Ohmura, A. 1998. Means and trends of shortwave irradiance at the surface estimated from Global Energy Balance Archive data. *J. Clim.* **11**, 2042–2061.

Gutowski, W. J., Gutzler, D. S. and Wang, W. C. 1991. Surface energy balances of three general circulation models: implications for simulating regional climate change. *J. Clim.* **4**, 121–134.

Halthore, R. N., Crisp, D., Schwartz, S. E., Anderson, G. P., Berk, A., and co-authors. 2005. Intercomparison of shortwave radiative transfer codes and measurements. *J. Geophys. Res.* **110**, D11206, doi:10.1029/2004JD005293.

Iacono, M. J., Mlawer, E. J., Clough, S. A. and Morcrette, J. J. 2000. Impact of an improved longwave radiation model, RRTM, on the energy budget and thermodynamic properties of the NCAR community climate model, CCM3. *J. Geophys. Res.* **105,** 14873–14890.

IPCC 2007. *Climate Change 2007: The Physical Science Basis* (Contribution of Working Group I to the Fourth Assessment Report of the Intergovernmental Panel on Climate Change) (eds S. Solomon, D. Qin, M. Manning, Z. Chen, M. Marquis and co-editors). Cambridge University Press, Cambridge, United Kingdom and New York, N.Y., USA, 996 pp.

Kato, S., Ackerman, T. P., Clothiaux, E.E, Mather, J. H., Mace, G. G. and co-authors. 1997. Uncertainties in modeled and measured clear-sky surface shortwave irradiances. *J. Geophys. Res.* **102**, 25881–25898.

Kinne, S., Bergstrom, R., Toon, O. B., Dutton, E. and Shiobara, M. 1998. Clear-sky atmospheric solar transmission: an analysis based on FIRE 1991 field experiment data. *J. Geophys. Res.* **103**, 19709–19720.

Li, Z., Whitlock, C. H. and Charlock, T. P. 1995. The variable effect of clouds on atmospheric absorption of solar radiation. *Nature* **376**, 486–490.

Li, Z., Moreau, L. and Arking, A. 1997. On solar energy disposition: a perspective from observation and modeling. *Bull. Am. Meteorol. Soc.* **78**, 53–70.

Li, Z., Trishchenko, A. P., Barker, H. W., Stephens, G. L. and Partain, P. 1999. Analyses of Atmospheric Radiation Measurement (ARM) program's Enhanced Shortwave Experiment (ARESE) multiple data sets for studyingcloud absorption. *J. Geophys. Res.*, **104**, 19127–19134.

Markovic, M., Jones, C., Vaillancourt, P., Paquin, D. and Paquin-Ricard, D. 2008. An evaluation of the surface radiation budget over North America for a suite of regional climate models and reanalysis data, Part 1: comparison to surface stations observations. *Clim. Dyn.* doi:10.1007/s00382-008-0378-6.

Morcrette, J.-J. 2002a. Assessment of the ECMWF model cloudiness and surface radiation fields at the ARM SGP site. *Mon. Wea. Rev.* **130**, 257–277.

Morcrette, J.-J. 2002b. The surface downward longwave radiation in the ECMWF forecast system. *J. Clim.* **15**, 1875–1892.

Ohmura, A., Gilgen, H. and Wild, M. 1989. Global energy balance archive GEBA, World Climate Program Project A7—Water, Report 1: Introduction, Zuercher Geografische Schriften Nr. 34, Verlag der Fachvereine, Zuerich, 62pp.

Ohmura, A., Dutton E. G., Frohlich C., Gilgen H., Hegner H. and co-authors. 1998. Baseline Surface Radiation Network (BSRN/WCRP), a new precision radiometry for climate research. *Bull. Am. Meteorol. Soc.* **79**, 2115–2136.

Ramanathan, V., Subasilar, B., Zhang, G., Conant, W., Cess, R. and co-authors. 1995. Warm pool heat budget and shortwave cloud forcing: a missing physics? *Science* **267**, 499–503.

Randall, D. A., Cess R. D., Blanchet J. P., Boer G. J., Dazlich D. A. and co-authors. 1992. Intercomparison and interpretation of surface energy fluxes in atmospheric general circulation models. *J. Geophys. Res.* **97**, 3711–3725.

Wild, M. 1999. Discrepancies between model-calculated and observed atmospheric shortwave absorption in areas with high aerosol loadings. *J. Geophys. Res.* **104**, 27361–27371.

Wild, M. 2000. Absorption of solar energy in cloudless and cloudy atmospheres over Germany and in GCMs. *Geophys. Res. Lett.* **27**, 959–962.

Wild, M. 2005. Solar radiation budgets in atmospheric model intercomparisons from a surface perspective. *Geophys. Res. Lett.* **32**, L07704, doi:10.1029/ 2005GL022421.

Wild, M. and Liepert, B. 1998. Excessive transmission of solar radiation through the cloud-free atmosphere in GCMs. *Geophys. Res. Lett.* **25**, 2165–2168.

Wild, M. and Roeckner, E. 2006. Radiative fluxes in ECHAM5. *J. Clim.* **19**, 3792–3809.

Wild, M., Ohmura, A., Gilgen, H. and Roeckner, E. 1995. Validation of GCM simulated radiative fluxes using surface observations. *J. Clim.* **8**, 1309–1324.

Wild, M., Dümenil, L. and Schulz, J. P. 1996. Regional climate simulation with a high resolution GCM: surface hydrology. *Clim. Dyn.* **12**, 755–774

Wild, M., Ohmura, A. and Cubasch, U. 1997. GCM-Simulated Surface Energy Fluxes in Climate Change Experiments. *J. Clim.* **10**, 3093–3110.

Wild, M., Ohmura, A., Gilgen, H., Roeckner, E., Giorgetta, M. and co-authors. 1998a. The disposition of radiative energy in the global climate system: GCM versus observational estimates. *Clim. Dyn.* **14**, 853–869.

Wild, M., Ohmura, A., Gilgen, H. and Morcrette, J. J. 1998b. The distribution of solar energy at the earth's surface as calculated in the ECMWF re-analysis. *Geophys. Res. Lett.* **25**, 4373–4376.

Wild, M., Ohmura, A., Gilgen, H., Morcrette, J. J. and Slingo, A. 2001. Evaluation of downward longwave radiation in general circulation models. *J. Clim.* **14**, 3227–3239.

Wild, M., Long, C. N. and Ohmura, A. 2006. Evaluation of clear-sky solar fluxes in GCMs participating in AMIP and IPCC-AR4 from a surface perspective. *J. Geophys. Res.* **111**, D01104, doi:10.1029/2005JD006118.